Revisions on egusphere-2025-4494.

The manuscript by Sanmiguel-Vallelado and colleagues “Unlocking the potential of pollarded oaks: A 375–year hydroclimate reconstruction from north central Spain” aims to presents a 375-year hydroclimate reconstruction based on pollarded deciduous oaks from communal dehesas in north-central Spain. The study is original and potentially important, showing that traditionally managed pollarded trees can retain a strong precipitation signal at stand level and can be used to reconstruct November–June hydroclimatic variability in a region where long lowland records are scarce (as some locations of Spain seem to be). The chronology is long, the latewood signal is robust, and the comparison with documentary drought evidence adds value. The overall premise is therefore compelling and timely.

However, at the same time, the manuscript would benefit from major revision before being considered for publication. The main concerns do not relate to novelty, but to some aspects of the reconstruction design and interpretation that require clearer justification (i.e. methodology). In particular, the pooling of two species and two sites into a single chronology, the calibration/validation framework based on different instrumental products, the use of quantile mapping, and the interpretation of extremes and pollarding effects all need more careful treatment.

Overall, the manuscript addresses an important gap in Mediterranean dendroclimatology by focusing on lowland dehesa systems and by highlighting pollarded oaks as a potentially valuable archive for hydroclimate reconstruction. Chronology statistics seem to be strong enough, with long RWI and LWI series and high EPS values, and the latewood index shows a clear relationship with November–June precipitation. The study also explores whether pollarding weakens the climate signal at the tree level and whether this propagates to the stand chronology. This is an interesting and useful contribution. The comparison with large-scale hydroclimate products and with rogation records further increases the relevance of the work.

However, several methodological choices underlying the reconstruction need stronger support.

Major comments:

Pooling of two species and two sites (only). The study combines Quercus faginea and Q. pyrenaica from two different woodlands into a single chronology. Although the sites are geographically close, they differ in species composition, and it is not fully demonstrated that pooling them does not blur the climate signal. Because the reconstruction relies on the pooled latewood chronology, separate site-level and species-level chronologies, together with their intercorrelations and climate responses, should be presented. Some references, if any, would strong these findings.

We agree that, when a reconstruction is based on a pooled chronology, it is important to verify that combining trees from different sites and species does not weaken or distort the target climatic signal. For this reason, before selecting the final predictor chronology, we compared the available site- and species-level latewood chronologies in terms of chronology quality, inter-correlation, and climate response.

These comparisons indicate that pooling trees did not blur the hydroclimatic signal. First, all subgroup latewood chronologies showed strong internal signal strength, with EPS values higher than 0.95 in every case and SNR values ranging from 18.24 to 31.27. The pooled chronology further increased robustness, reaching EPS = 0.97 and SNR = 31.27. Thus, the combined chronology provides the strongest overall common signal among the alternatives considered.

Second, the subgroup chronologies were strongly correlated with the pooled chronology. Pearson’s correlation coefficients between the pooled chronology and the subgroup chronologies were 0.84 for VA, 0.98 for VI, 0.86 for QP, and 0.98 for QF. These high values show that the pooled series captures the same dominant interannual variability already present in the separate site- and species-level chronologies, rather than generating an artificial mixed signal.

Third, and most importantly, all subgroup chronologies showed a highly consistent climate response. In every case, the maximum Pearson correlation with instrumental precipitation was obtained for the same target season, November–June. Correlation coefficients were similar across subsets: 0.83 for QF, 0.76 for QP, 0.74 for VA, 0.84 for VI, and 0.84 for the pooled chronology. Therefore, pooling did not alter the target seasonal hydroclimatic signal; instead, it retained the same signal while increasing sample depth and chronology robustness.

Based on these results, we consider the pooled latewood chronology to be the most appropriate predictor for reconstruction. It preserves the common signal shared among trees from both sites and species, while providing the highest replication and the strongest overall chronology statistics. This selection criterion is consistent with standard dendrochronological practice, in which multiple candidate chronologies are screened and the final published chronology is the one that maximizes replication and common signal strength once coherence among candidate subsets has been verified (e.g. Cooper et al. 2011, Clim Dyn, doi:10.1007/s00382-012-1328-x; Frank & Esper 2004, Dendrochronologia, doi:10.1016/j.dendro.2005.02.004).

We have therefore clarified this decision in the Methods section. However, we did not incorporate all of these routine screening checks into the supplementary material, because they correspond to the standard chronology-selection procedure used to define the final chronology reported in the manuscript, rather than to independent result sections. We appreciate the reviewer's concern, since these additional comparisons were useful to further verify the robustness of the selected chronology.

Table X. Descriptive statistics of the five latewood chronologies: all trees, VI (Vilviestre), VA (Valonsadero), QF (Quercus faginea), and QP (Quercus pyrenaica). AR1 denotes first-order autocorrelation. RBAR, SNR, and EPS were calculated from detrended series.

Chronology	N trees	Site	Species	Period of EPS > 0.85	Chron. length	Mean width (mm)	SD width (mm)	Mean AR1	RBAR	SNR	EPS
All	**102**	**VA, VI**	**QF, QP**	**1649**	**375**	**0.39**	**0.35**	**0.47**	**0.24**	**31.27**	**0.97**
VA	40	VA	QP	1843–2022	181	0.60	0.48	0.41	0.32	19.18	0.95
VI	62	VI	QF, QP	1649–2023	375	0.26	0.11	0.51	0.25	20.08	0.95
QP	45	VA, VI	QP	1843–2022	181	0.57	0.46	0.41	0.31	19.72	0.95
QF	57	VI	QF	1649–2023	375	0.25	0.09	0.52	0.24	18.24	0.95

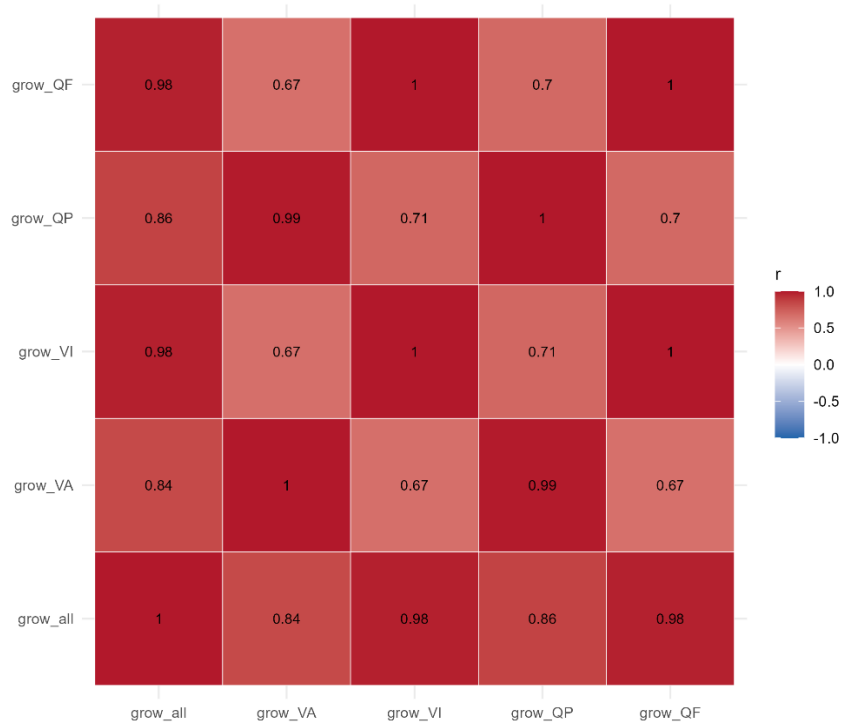

Figure X. Pearson's correlation coefficients among the five latewood chronologies: all trees, VI (Vilviestre), VA (Valonsadero), QF (Quercus faginea), and QP (Quercus pyrenaica).

Table X. Maximum Pearson's correlation between the five latewood chronologies (all trees, VI: Vilviestre, VA: Valonsadero, QF: Quercus faginea, QP: Quercus pyrenaica) and FIC precipitation for the period 1952–2020.

Chronology	Month or season	r	CI_lower	CI_upper	Significant (p < 0.05)
QF	Nov-Jun	0.83	0.78	0.89	TRUE
QP	Nov-Jun	0.76	0.66	0.83	TRUE
VA	Nov-Jun	0.74	0.64	0.83	TRUE
VI	Nov-Jun	0.84	0.77	0.89	TRUE
All trees	**Nov-Jun**	**0.84**	**0.78**	**0.88**	**TRUE**

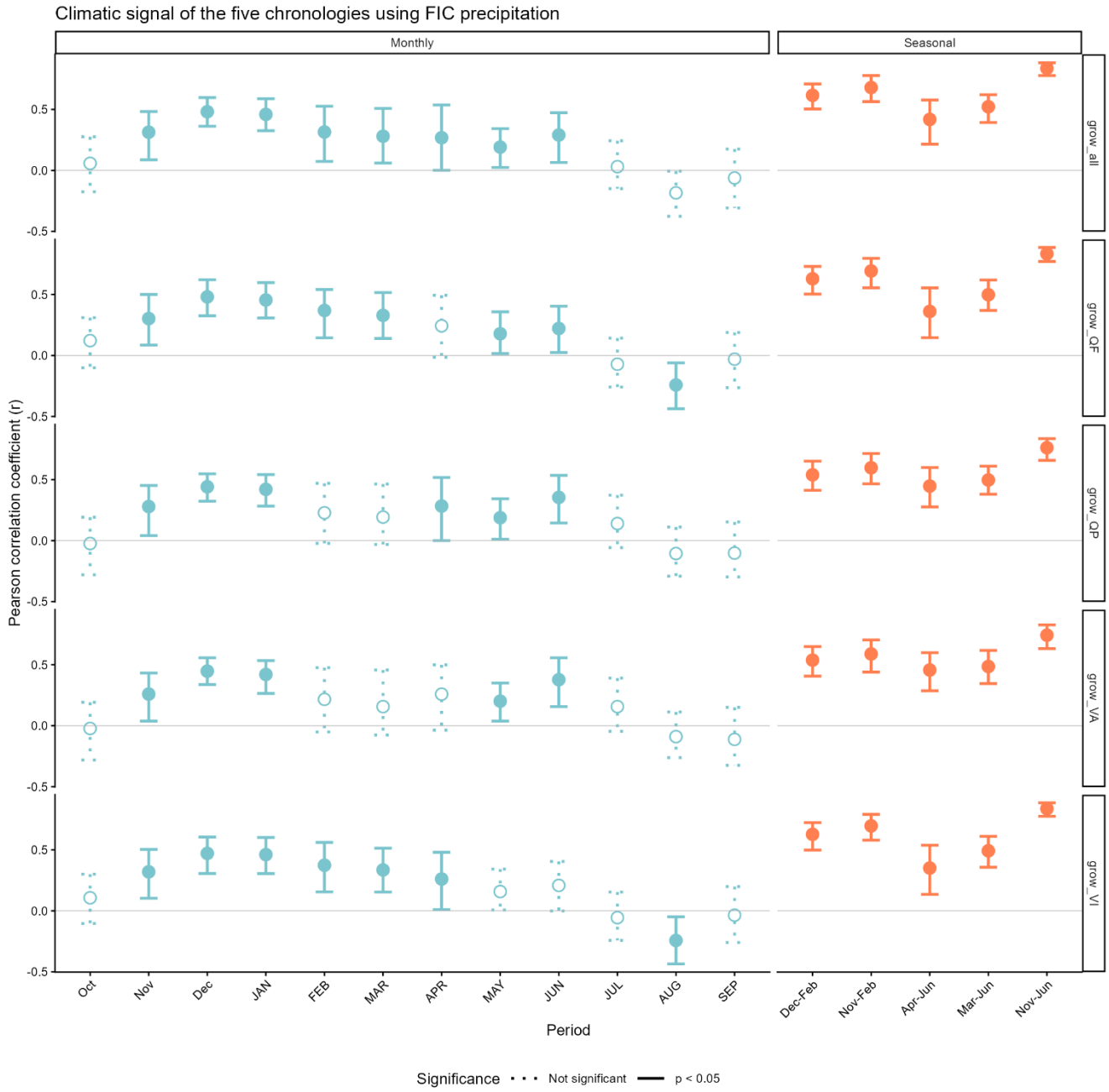

Figure X. Monthly and seasonal Pearson's correlation coefficients between the five latewood chronologies (all trees, VI: Vilviestre, VA: Valonsadero, QF: Quercus faginea, QP: Quercus pyrenaica) and FIC precipitation for 1952–2020. Monthly correlations were calculated from October of the previous year to September of the current year.

The reconstruction is calibrated using FIC precipitation and validated against CRU. While understandable, using different datasets for calibration and validation makes it difficult to interpret model skill. A more standard approach would strengthen the results, **such as** split-period calibration/verification using a single dataset, parallel tests with both datasets, or cross-validation (e.g. leave-one-out).

During the model development stage, we tested a single-dataset split-period calibration/verification approach with CRU and FIC separately, following one of the standard strategies suggested by the reviewer. At that stage, we retained the late FIC calibration (1962–2020) and early CRU validation (1902–1961) scheme because we considered it the most stringent among the tested alternatives. By calibrating and validating the reconstruction against two independent instrumental products, this framework provided a more demanding test of the stability and robustness of the climate–growth relationship than approaches based on a single dataset alone.

We agree, however, that presenting these additional tests in the manuscript improves the transparency and interpretability of model skill. We have therefore now included a summary table of all tested calibration–validation schemes in the Supplement (Table S7), and revised the Methods and Results sections accordingly.

Table S7: Calibration–validation schemes tested for the November–June precipitation reconstruction.

Scheme	CALIBRATION			VALIDATION					
	Calibration dataset	Calibration period	Adjusted R^2	Validation dataset	Validation period	r	RE	CE	RMSE (mm)
Late FIC calibration – Early CRU validation	FIC	1962–2020	0.70	CRU	1902–1961	0.71	0.44	0.45	76.21
Late CRU calibration – Early CRU validation	CRU	1962–2022	0.69	CRU	1902–1961	0.71	0.44	0.45	76.21
Early CRU calibration – Late CRU validation	CRU	1902–1961	0.48	CRU	1962–2022	0.83	0.67	0.67	53.75
Early FIC calibration – Late FIC validation	FIC	1952–1986	0.67	FIC	1987–2020	0.84	0.68	0.68	77.60

Note: adjusted R^2 = adjusted coefficient of determination; r = Pearson's correlation coefficient; RE = reduction of error; CE = coefficient of efficiency; RMSE = root-mean-square error.

Quantile mapping is applied to correct distributional biases and better capture extremes. Since the manuscript emphasizes extreme years and prolonged wet/dry periods, this step is important and should be better justified. It should be clarified whether the analysis of extremes is based on the raw or bias-corrected series, and how sensitive the results are to this correction.

We agree that the quantile-mapping step required clearer justification. We have now clarified in the revised manuscript that the analysis of extreme years is based on the bias-corrected reconstruction, as this series provides the closest match to the distribution of the instrumental CRU target over the common period.

We also evaluated the sensitivity of extreme-year detection to the correction step by comparing the raw and bias-corrected reconstructions using three thresholding approaches: a fixed ±1.5 SD threshold, the 5th/95th percentiles, and an Standardized Precipitation Index (SPI)-based classification. This comparison shows that most extreme years are robust to the correction, with 40 events identified in both reconstructions. However, the correction does affect the classification of some individual years: 8 dry extremes were identified only in the raw reconstruction, whereas 12 wet extremes were identified only in the bias-corrected reconstruction. This comparison indicates that the correction mainly affects marginal cases near the thresholds, whereas the most pronounced extremes are largely consistent between the raw and bias-corrected reconstructions.

Nevertheless, because the bias-corrected reconstruction more faithfully reproduces the variability and distribution of the instrumental target series, we consider it the most appropriate version for the identification and interpretation of extreme wet and dry years. To make this sensitivity transparent, we have included in the Supplement the lists of extreme years identified in the raw and bias-corrected reconstructions (Table S8).

Table S8: Extreme years identified in the raw and bias-corrected precipitation reconstructions, indicating detection agreement between reconstructions, identifying method(s), reconstructed precipitation in both series, and Standardized Precipitation Index (SPI) values. Dry years are ordered from lower to higher precipitation and wet years from higher to lower precipitation.

Extreme type	Year	Detected in both reconstructions?	Method(s)	Bias-corrected precipitation (mm)	Raw precipitation (mm)	SPI
Dry	1683	Yes	mean-1.5 SD; P5; SPI	257	273	-1.92
	1734	Yes	mean-1.5 SD; P5; SPI	258	275	-2.09
	2012	Yes	mean-1.5 SD; P5; SPI	265	287	-1.70
	1995	Yes	mean-1.5 SD; P5; SPI	276	303	-1.66
	2005	Yes	mean-1.5 SD; P5; SPI	276	304	-1.88
	1737	Yes	mean-1.5 SD; P5; SPI	288	322	-1.67
	1775	Yes	mean-1.5 SD; P5; SPI	288	322	-1.93
	1999	Yes	mean-1.5 SD; P5; SPI	290	325	-1.83
	1868	Yes	mean-1.5 SD; P5	290	325	-1.42
	1981	Yes	P5; SPI	294	331	-1.58
	1698	Yes	P5; SPI	295	334	-1.54
	1949	Yes	P5; SPI	296	335	-1.96
	1738	Yes	P5	298	337	-1.41
	1898	Yes	P5; SPI	298	338	-1.56
	1767	Yes	P5	303	346	-1.30
	1718	Yes	P5	304	348	-1.47
	1844	Yes	P5	305	349	-1.26
	1665	Yes	P5	312	360	-1.32
	1833	Yes	P5	315	364	-1.28
	1803	No (raw only)	mean-1.5 SD	316	366	-1.14
	1687	No (raw only)	SPI	318	369	-1.44
	1699	No (raw only)	SPI	319	370	-1.43
	1744	No (raw only)	SPI	320	372	-1.46
	1828	No (raw only)	SPI	324	377	-1.42
	1811	No (raw only)	SPI	327	383	-1.38
	1896	No (raw only)	SPI	329	385	-1.40
	1757	Yes	SPI	329	385	-1.50
	1824	No (raw only)	SPI	329	386	-1.39
Wet	1684	Yes	mean+1.5 SD; P95; SPI	838	857	3.01
	1784	Yes	mean+1.5 SD; P95; SPI	771	804	2.19

1988	*Yes*	*mean+1.5 SD; P95; SPI*	*754*	*791*	*2.10*
1708	*Yes*	*mean+1.5 SD; P95; SPI*	*750*	*788*	*2.41*
1966	*Yes*	*mean+1.5 SD; P95; SPI*	*748*	*786*	*2.58*
1930	*Yes*	*mean+1.5 SD; P95; SPI*	*734*	*775*	*2.48*
1977	*Yes*	*mean+1.5 SD; P95; SPI*	*711*	*757*	*2.84*
1692	*Yes*	*mean+1.5 SD; P95; SPI*	*711*	*757*	*2.16*
1800	*Yes*	*mean+1.5 SD; P95; SPI*	*676*	*730*	*1.90*
1795	*Yes*	*mean+1.5 SD; P95; SPI*	*674*	*728*	*2.19*
1736	*Yes*	*mean+1.5 SD; P95*	*664*	*721*	*1.56*
1799	*Yes*	*mean+1.5 SD; P95; SPI*	*657*	*715*	*2.00*
1848	*Yes*	*mean+1.5 SD; P95*	*629*	*693*	*1.53*
2021	*Yes*	*mean+1.5 SD; P95; SPI*	*628*	*692*	*1.68*
1814	*Yes*	*mean+1.5 SD; P95; SPI*	*626*	*690*	*2.15*
1735	*Yes*	*mean+1.5 SD; P95; SPI*	*624*	*689*	*1.78*
1763	*Yes*	*mean+1.5 SD; P95*	*605*	*674*	*1.56*
1731	*Yes*	*mean+1.5 SD; P95*	*603*	*673*	*1.66*
1670	*Yes*	*mean+1.5 SD; P95; SPI*	*601*	*671*	*1.92*
1860	*No (bias-corrected only)*	*mean+1.5 SD*	*600*	*670*	*1.29*
1721	*No (bias-corrected only)*	*mean+1.5 SD*	*596*	*667*	*1.40*
1762	*No (bias-corrected only)*	*mean+1.5 SD*	*596*	*667*	*1.47*
1758	*Yes*	*SPI*	*594*	*666*	*1.74*
1877	*No (bias-corrected only)*	*mean+1.5 SD*	*589*	*662*	*1.34*
1985	*No (bias-corrected only)*	*mean+1.5 SD*	*588*	*660*	*1.32*
1915	*No (bias-corrected only)*	*mean+1.5 SD*	*586*	*659*	*1.44*
1746	*No (bias-corrected only)*	*SPI*	*583*	*657*	*1.64*
1782	*No (bias-corrected only)*	*SPI*	*569*	*646*	*1.51*
2013	*No (bias-corrected only)*	*SPI*	*568*	*646*	*1.59*
1969	*No (bias-corrected only)*	*SPI*	*539*	*622*	*1.68*
1861	*No (bias-corrected only)*	*SPI*	*535*	*619*	*1.64*
1657	*No (bias-corrected only)*	*SPI*	*528*	*613*	*1.56*

The manuscript concludes that pollarding does not affect the stand-level signal. This is plausible, but the evidence is limited (again, some additional references would strong the findings of the MS). The argument appears to rely on asynchronous pollarding among trees, yet the temporal distribution of pollarding events is not quantified. Providing a summary of the proportion of trees affected through time would strengthen this conclusion.

We agree that the conclusion about pollarding not obscuring the stand-level climate signal is stronger when the temporal distribution of pollarding events is explicitly quantified. In response, we added a new supplementary figure (Fig. S4) showing the percentage of trees affected by pollarding through time, following the event-detection approach of Sanmiguel-Vallelado et al. (2024).

The new figure shows that pollarding was markedly asynchronous across trees in both dehesas: 75% of pollarding events affected less than 6% of the available trees, and only three events exceeded 30% synchrony (1697, 1736 and 1800, with 36.4%, 30.6% and 31.7% of trees affected, respectively). This quantification supports our interpretation that management effects were generally diluted at the stand level because most pollarding events involved only a small fraction of trees at any given time.

We have revised the manuscript text to make this argument more explicit and less categorical. Rather than stating that pollarding does not affect the stand-level signal in absolute terms, we now indicate that the common hydroclimatic signal can be preserved when pollarding is sufficiently asynchronous among trees. To our knowledge, Olano et al. (2023), which is already cited in the manuscript, is the only previous study

explicitly addressing the effect of pollarding on the stand-level climate signal. Their results suggest that pollarded oak chronologies can retain a substantial common climate signal under asynchronous management, whereas stronger synchrony in management may leave a clearer stand-level imprint in tree-ring series. Our new Fig. S4 provides a quantitative summary of pollarding asynchrony in our sites and therefore reinforces this interpretation.

This interpretation is also supported by the chronology statistics. RBAR, which represents the mean correlation among all individual series, is expected to be reduced when pollarding events occur asynchronously and introduce tree-specific growth disturbances in different years. In contrast, Series IC, which measures the correlation of each series with the common residual chronology, remains high when a shared climatic signal is retained despite such noise. This pattern is evident in the series retained for reconstruction (1949–2023): RBAR is relatively low (0.21), whereas Series IC is high (0.50). This pattern is consistent with the rotational and asynchronous pollarding regime of these stands and supports the conclusion that management effects were largely diluted at the stand level, allowing the common hydroclimatic signal to remain dominant.

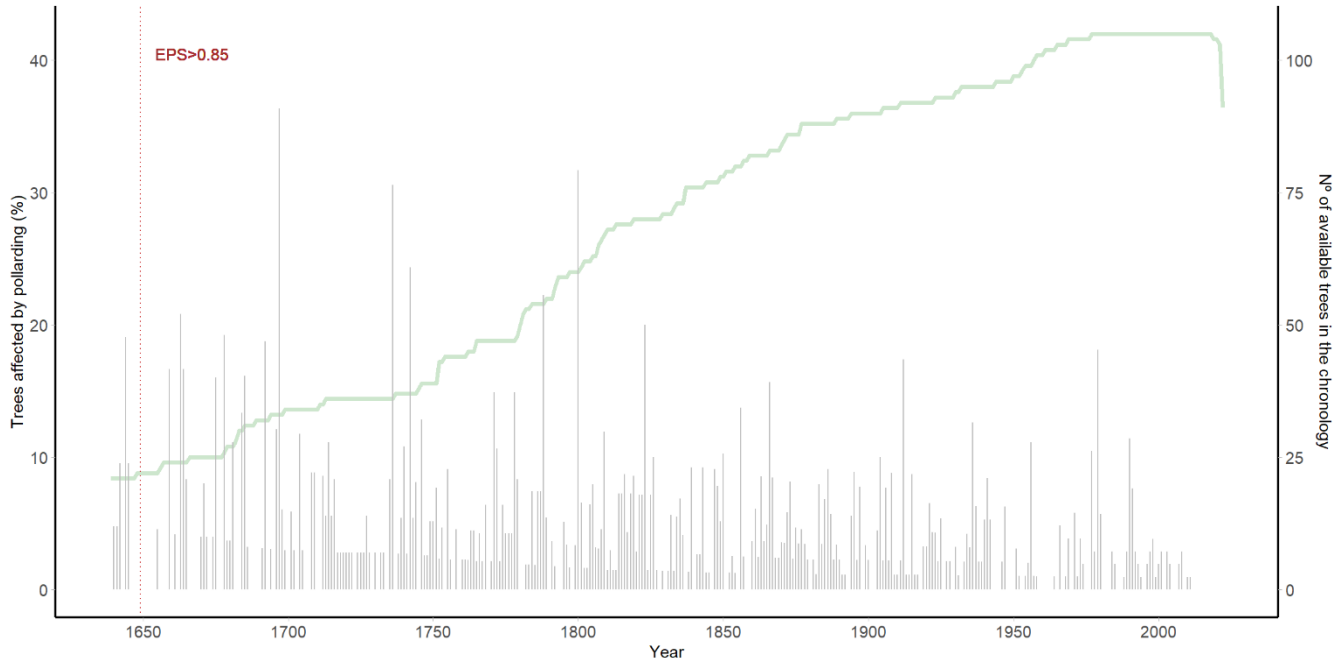

Figure S4. Percentage of trees affected by pollarding events each year (grey segments) relative to the number of trees available in the chronology at that time (green line), based on Sanmiguel-Vallelado et al. (2024).

In addition, extreme years and prolonged wet/dry periods are defined using fixed thresholds. Because these results are central to the manuscript, a short sensitivity analysis using alternative thresholds would be useful.

We agree that the definition of extreme years should not rely on a single threshold criterion, particularly because these results are central to the manuscript. We have therefore added a short sensitivity analysis using two alternative approaches in addition to the original ±1.5 SD threshold: a percentile-based criterion (5th/95th percentiles) and a Standardized Precipitation Index (SPI)-based classification. The revised manuscript now includes this comparison in the Methods and Results sections (revised Fig. 6), as well as in the Supplementary Material (new Table S8 and new Fig. S12).

The results show that extreme wet and dry years identified from the bias-corrected reconstruction are broadly consistent across the three threshold criteria. For dry extremes, eight years were common to all three methods (1683, 1734, 1737, 1775, 1995, 1999, 2005, and 2012), highlighting them as the most robust drought events in the reconstruction. For wet extremes, agreement was even stronger, with 19 years identified by all three methods (1670, 1684, 1692, 1708, 1731, 1735, 1736, 1763, 1784, 1795, 1799, 1800, 1814, 1848, 1930, 1966, 1977, 1988, and 2021). Although additional events were detected only by one or two methods, the main

temporal pattern remained unchanged, with dry extremes concentrated in the 1730s and during the late 20th to early 21st centuries, and wet extremes particularly frequent between the 1730s and 1800, with additional peaks during the 20th century.

Importantly, the historical support for reconstructed droughts also proved robust to threshold choice. All extremely dry years identified under the different criteria were supported by documentary evidence, including pro pluvia rogation records and/or catalogue-based historical drought records. We believe that this additional sensitivity analysis strengthens the manuscript by showing that the main hydroclimatic patterns discussed are not dependent on a single fixed threshold, while also making explicit which individual years are most robust across alternative definitions of extremes.

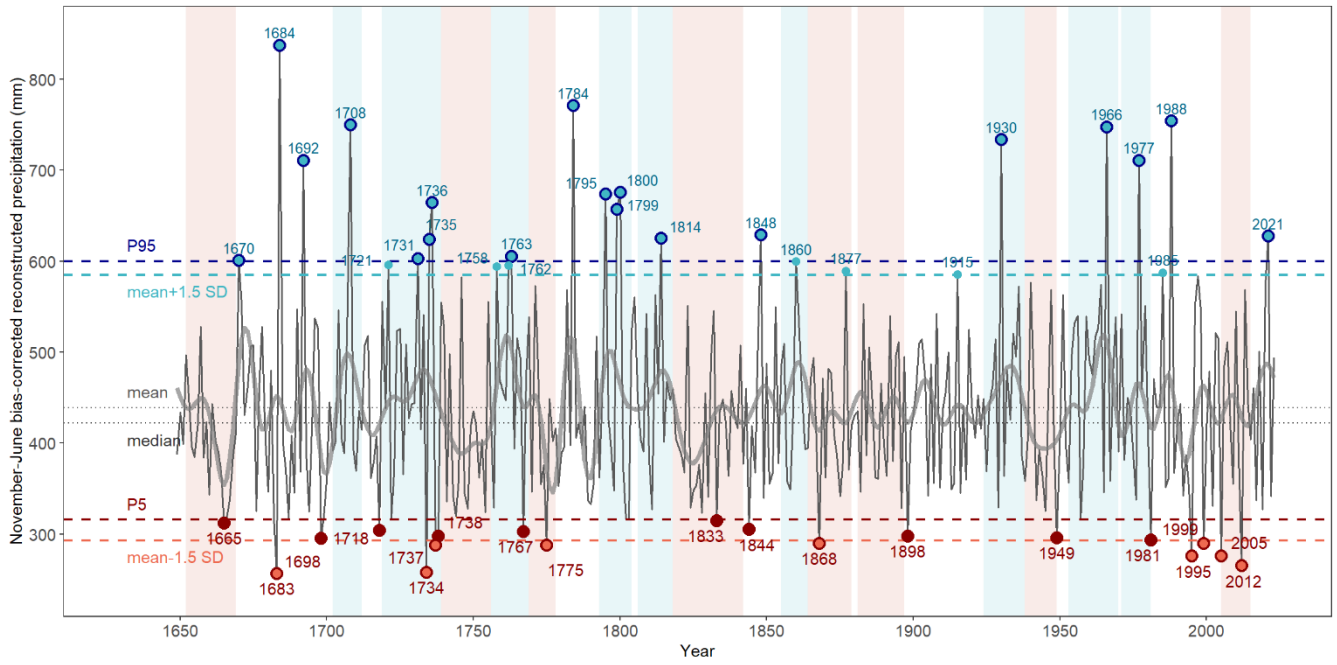

Figure 6: Reconstructed November–June precipitation from 1649-2023 based on pollarded oak LWI data. Shaded areas indicate wet (blue) and dry periods (red), while extreme wet and dry years are marked with blue and red dots, respectively. Thick curve is a 10-year low-pass filter.

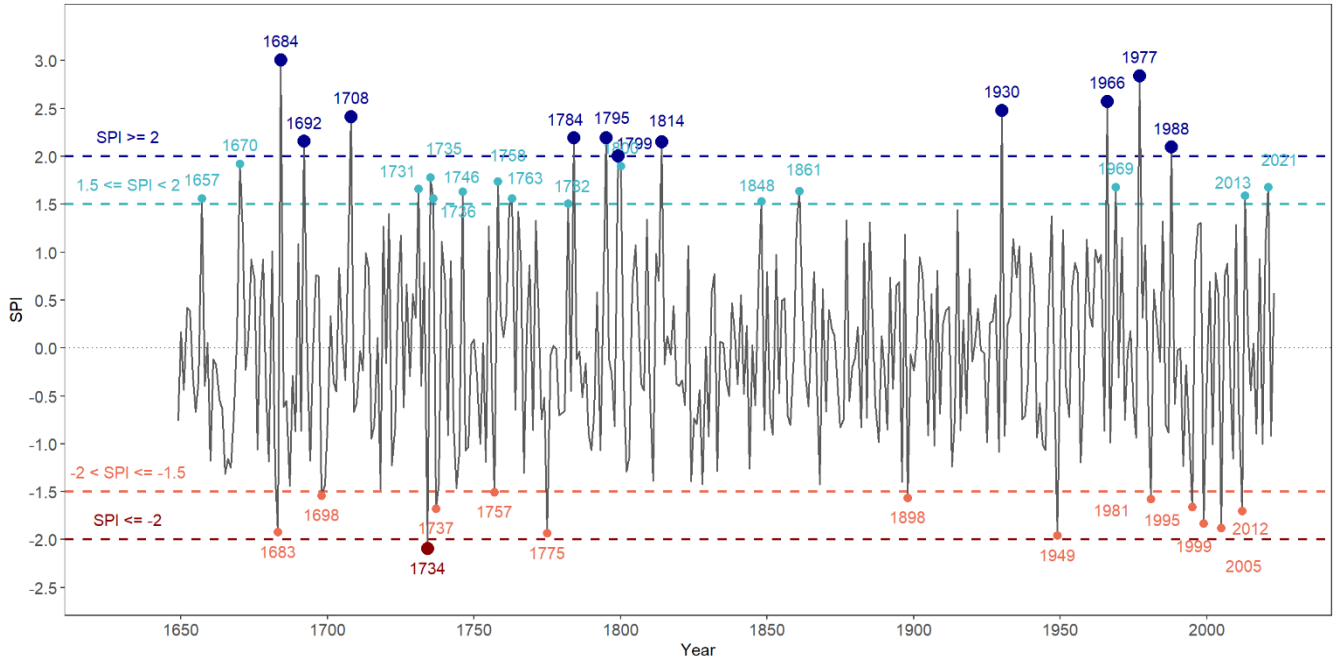

Figure S12: Extreme wet and dry years identified in the bias-corrected November–June precipitation reconstruction (1649–2023) using SPI categories.

Rogation records come from surrounding locations rather than from the study sites. The comparison is useful, but the interpretation should be framed more cautiously as regional coherence rather than direct local validation.

We agree that the rogation records do not provide direct local validation, as no such records are available for the study sites. As stated in the manuscript, we therefore used the closest available locations, selected on the basis of both geographic proximity and shared climatic patterns (see Fig. 2). We consider that agreement at this broader spatial scale supports the regional representativeness and robustness of the reconstruction and provides evidence of strong regional coherence. Importantly, the fact that the reconstruction agrees with independent documentary evidence beyond the immediate study sites reinforces its robustness and supports the regional representativeness of the hydroclimatic signal captured by the chronology.

In the pre-print, the rogation localities shown in Fig. 2 were located within the area of high spatial field correlation between CRU November–June precipitation and the chronology. These points were moved to Fig. 1a in the revised version following Reviewer 1's suggestion but this does not alter the interpretation: agreement at this broader spatial scale reinforces the regional representativeness and robustness of the reconstruction.

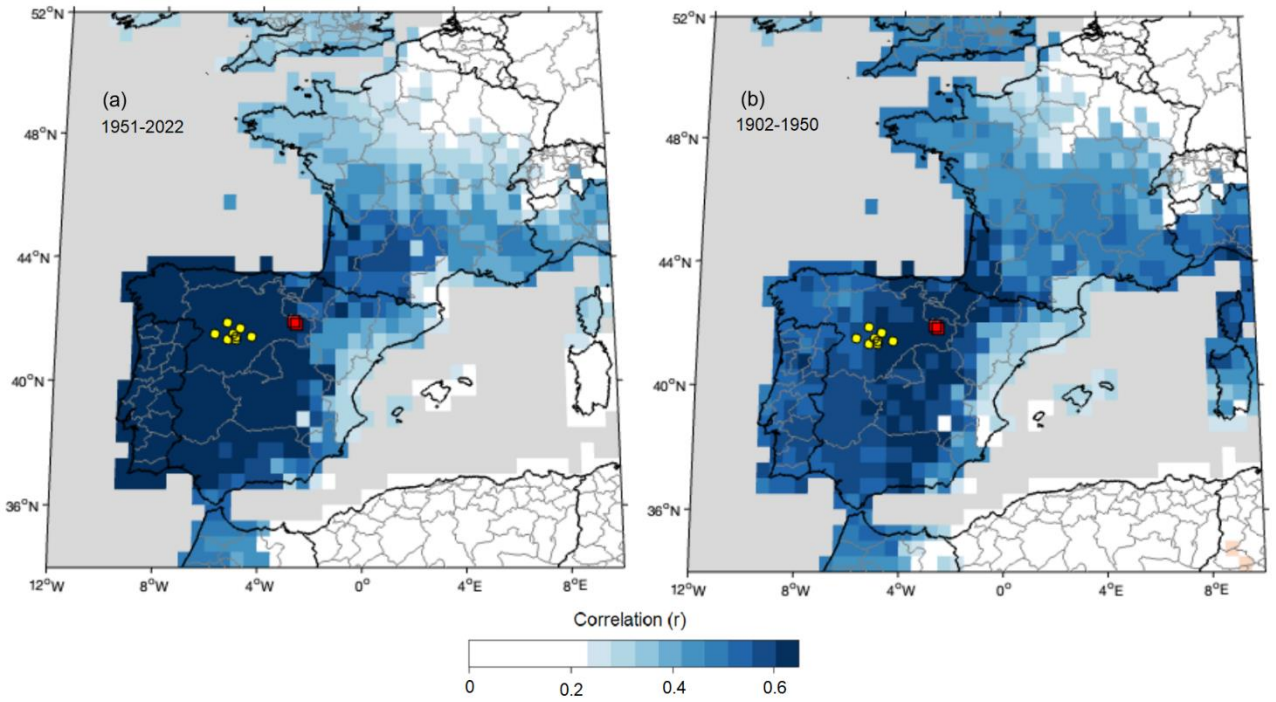

Figure 2 (pre-print version): Spatial field correlations (p < 0.05) between November–June precipitation (CRU) and the LWI chronology for two periods: (a) 1951–2022 and (b) 1902–1950. Yellow dots indicate the locations of the towns where *pro pluvia* rogation ceremonies were held, used here to validate extremely dry years. Red squares indicate the locations of the Vi and Va sampled *dehesas*.

The manuscript indicates that data and code will be available upon request. Public archiving of chronologies, reconstruction data, and code would improve reproducibility and long-term usefulness.

We thank the reviewer for this suggestion and agree that public archiving would improve the reproducibility and long-term usefulness of the study. We will therefore deposit both the chronology and the reconstructed precipitation series in a public repository upon acceptance of the manuscript, and we will revise the Data Availability statement accordingly. All analyses were conducted in R using open-source packages, as indicated in the Methods section, which ensures that the analytical tools employed are already publicly accessible.

Some minor comments:

Section numbering in the Methods appears inconsistent (Section 2.4 missing).

Done. Section numbering has been corrected.

Several language issues and typos should be corrected.

Thank you. The manuscript has been carefully revised to correct language issues and typographical errors throughout.

The final regression equation should be reported explicitly.

We have now reported the final regression equation explicitly in the Results section. The final transfer function is: November–June precipitation (mm) = 154.59 + 379.77 × LWI.

Since only one core per tree was extracted, potential implications for within-tree variability should be discussed more clearly.

We agree that using more than one core per tree would allow a better quantification of within-tree variability related to uneven radial growth, cambial heterogeneity, mechanical stress, or microsite effects. In this study, however, we prioritized sampling a large number of trees in order to maximize the population-level common signal, rather than extracting multiple cores from fewer individuals. This strategy is consistent with standard dendrochronological principles, according to which chronology signal strength depends strongly on replication, and with previous work on pollarded oaks showing that one core per tree can be preferable when the aim is to reduce the redundancy of management signals within individuals while maximizing the number of sampled trees.

We acknowledge that within-tree variability was not explicitly quantified here and therefore remains a source of uncertainty. However, the large sample depth (>100 trees) and the high EPS values of both RWI and LWI chronologies (>0.90 since 1664) indicate that the mean chronology captures a strong common signal despite this unquantified source of variance. To address this point more clearly, we have revised the Methods section to explain the rationale behind our sampling design and explicitly acknowledge its limitation for quantifying within-tree variability. The following text has been added: "Given the low competition and strong common signal among trees in the dehesas, we extracted only one core per tree using a Pressler increment borer (Olano et al., 2023). This sampling strategy prioritized the number of sampled individuals over multiple cores per tree in order to maximize the population-level common signal and avoid redundant management signals within the same individual. Although this design does not explicitly quantify within-tree growth variability, the large sample depth helps dilute individual-level noise in the mean chronology."

The discussion of latewood performance could be linked more directly to the empirical results.

We agree that the discussion of latewood performance should be linked more explicitly to the empirical interpretation behind it. In our previous work on the same system, we showed that pollarding effects are expressed mainly through sharp reductions in latewood, whereas earlywood remains comparatively less affected in the first years after management (Sanmiguel-Vallelado et al., 2024). This does not reduce the climatic value of latewood. On the contrary, in ring-porous oaks latewood is formed later in the growing season, when radial growth depends more directly on current water availability, whereas earlywood formation is initiated earlier and can rely more strongly on previously stored resources. Therefore, latewood is the ring component in which both management and drought signals are most strongly expressed. We have

revised the Discussion to clarify this point and to explain that the good hydroclimatic performance of latewood at stand level is most likely related to its strong sensitivity to water availability, while management effects are diluted in the mean chronology because pollarding is markedly asynchronous among trees.